

Superconducting dome in ferroelectric-type materials from soft mode instability

Chandan Setty*

Department of Physics and Astronomy, Rice Center for Quantum Materials, Rice University, Houston, Texas 77005, USA

Matteo Baggioli†

*Wilczek Quantum Center, School of Physics and Astronomy,
Shanghai Jiao Tong University, Shanghai 200240,
China & Shanghai Research Center for Quantum Sciences, Shanghai 201315.*

Alessio Zacccone‡

*Department of Physics “A. Pontremoli”, University of Milan, via Celoria 16, 20133 Milan, Italy. and
Cavendish Laboratory, University of Cambridge, JJ Thomson Avenue, CB30HE Cambridge, U.K.*

We present a minimal theory of superconductivity enhancement in ferroelectric-type materials. Simple expressions for the optical mode responsible for the soft mode transition are assumed. A key role is played by the anharmonic phonon damping which is modulated by an external control parameter (electron doping or mechanical strain) causing the appearance of the soft mode. It is shown that the enhancement in the superconducting critical temperature T_c upon approaching the ferroelectric transition from either side is due to the Stokes electron-phonon scattering processes promoted by strong phonon damping effects.

I. INTRODUCTION

Although it was originally thought that ferroelectricity and ferroelectric-type crystals cannot support superconductivity¹, connections between the two phenomena were explored^{2–4} early on, and a possible origin of superconductivity was understood in terms of dielectric screening⁵ on the pairing mechanism or the role of ferroelectric instabilities⁶. Since then, a number of systems have been discovered where superconductivity may coexist with a quantum critical ferroelectric transition^{7,8}, and where the presence of the soft mode appears to enhance the superconducting critical temperature T_c . Most notably, this is the case of strontium titanate, SrTiO_3 , for which several conventional and unconventional mechanisms have been discussed^{4,9,10} since its early discovery¹¹. Even though the unusual conditions due to extreme dilution of electrons make the pairing mechanism in SrTiO_3 still a highly debated topic, a basic BCS framework can be applied to extract qualitative pairing trends.^{12,13}

More recently, enhanced superconductivity domes in the proximity of soft mode instabilities, induced by electron doping¹⁴ and mechanical strain¹⁵, have been observed. The role of structural instability in promoting superconductivity is suggested by the recent finding that plastic mechanical deformations appear to further enhance superconductivity possibly due to self-organized dislocation networks¹⁶. Various theoretical explanations^{10,15,17–19} have been proposed to understand such effects in these ferroelectric-type materials, although a complete picture of the mechanism of T_c enhancement near the instabilities is unclear.

The role of structural instability, and its influence on superconductivity, similar to what happens in ferroelectrics²⁰, is also a highly debated topic in the context of high-temperature superconductors, both

cuprates^{21,22} and the recently discovered hydrides under high pressure^{23–25}, and, in general, in strongly coupled superconductors²⁶. For example, it is well known that, before the discovery of cuprates, high- T_c superconductivity was sought in A15 intermetallic compounds which exhibit soft-mode structural instability²⁷. While soft mode instabilities and phonon softening have been observed in several cuprates^{28–32} always below the T_c ³³, their role in promoting superconductivity remains uncertain²⁴.

In all the relevant experimental systems^{10,14,15,34} the anharmonic phonon damping plays a key role²⁴, which is reflected in gigantic values of the Grüneisen parameter as recently observed in Ref.¹⁵. If the soft mode is induced by electron doping, the damping arises from the enhanced electron-phonon coupling; if, instead, it is induced by mechanical strain, the damping is increased by the sheer interatomic potential anharmonicity as the strain pushes atoms away from the harmonic part of the bonding wells.

Hence, it is imperative to understand the effect of the soft mode on superconductivity by directly considering the effect of the growing anharmonic phonon damping accompanying the soft mode instability. From the perspective of effective theories, we proposed a minimal theoretical model based on the anharmonically extended BCS theory^{35,36}, which includes the effect of anharmonic damping of phonons mediating the superconductivity. In this work, we demonstrate that the superconducting dome in ferroelectric-type materials, or, more generally, systems with soft-mode structural instabilities, originates from the enhancement of the superconducting critical temperature T_c due to anharmonic phonon damping that peaks at the instability point. An analogue of this effect, in the absence of soft mode instabilities, was recently predicted theoretically³⁵ and was found to be consistent with recent experimental observations³⁷.

II. THEORETICAL FRAMEWORK

A. Soft mode description

We start by assuming an optical phonon undergoing a ferroelectric-type soft mode transition as a function of a generic external control parameter n , which could be e.g. mechanical strain or electron doping. The external control parameter acts on the complex optical dispersion relation by affecting the phonon damping, i.e. by increasing it up to the point where the phonon energy vanishes and the soft mode is created.

In general, at low enough values of the frequency ω and the wave-vector k , within the so-called *hydrodynamic expansion*, the optical phonon dispersion relation satisfies³⁸

$$-\omega^2 + \omega_0^2 - i\omega\Gamma = 0 \quad (1)$$

where ω_0 is the phonon frequency (already renormalized by anharmonicity) and Γ is the anharmonic phonon damping, which is quantitatively related to the Grüneisen coefficient¹⁵ via the Klemens relation³⁹. Here, higher corrections in the wave-vector are ignored for simplicity. In ferroelectric-type materials the optical phonon that undergoes the softening is typically the transverse optical (TO) phonon⁴⁰, and therefore its coupling to electronic degrees of freedom is weak or negligible due to the vanishing of the dot product^{18,41}. Recent work^{42,43} (see also Ref.¹⁹) showed that, in reality, a significant coupling of the soft TO phonon to electrons can be induced by Rashba effects due to spin-orbit coupling. Other mechanisms have been also proposed which can enhance the coupling^{44–47}. In our effective model, we remain agnostic as to the origin of the coupling of the soft optical phonon to the electrons and we instead focus on the role of anharmonic damping connected with the softening.

The presence of the damping $\Gamma > 0$ causes both a renormalization of the natural (bare) phonon energy, the real part of the frequency ω appearing in Eq.(1), which becomes:

$$\text{Re}(\omega) = \frac{1}{2} \sqrt{4\omega_0^2 - \Gamma^2} < \omega_0, \quad (2)$$

as well as the finite lifetime $\tau = (\Gamma/2)^{-1}$ (its imaginary part). Both these effects can be computed for a given lattice structure and interatomic interactions via Self-Consistent Phonon (SCP) theory^{48–50} by considering three and four-phonon processes, i.e. by accounting for anharmonicity of the lattice. Here, we shall assume that the damping Γ is also a function of an additional external degree of freedom, which could be mechanical strain or electron doping. In the former case, varying the mechanical strain causes the atoms to sample more anharmonic parts of the interaction potential. In the latter case, electronic doping changes the electron-phonon damping which also contributes to Γ .

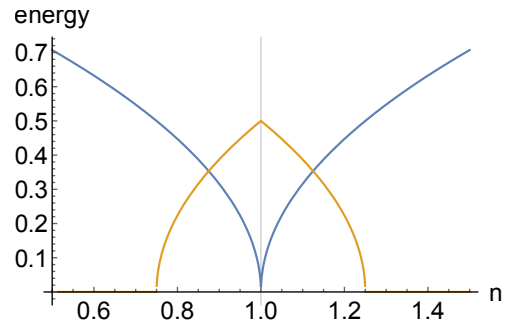


FIG. 1. Simplified model expressions for the optical mode energy (blue) and the inverse lifetime τ^{-1} (orange) upon approaching the soft mode instability as a function of a generic control parameter n . Here, $\omega_0 = 0.5$, $n_c = 1$.

We consider an effective description and we remain agnostic about the exact nature of the microscopic processes that change Γ as our goal is to have a generic model to study how variations in Γ induced by a generic external parameter n lead to changes in the superconducting T_c . We assume the existence of a soft mode instability (ferroelectric-type transition) characterized by the typical Curie-Weiss behavior as a function of an external control parameter n :

$$\text{Re}(\omega) = \sqrt{|n_c - n|}. \quad (3)$$

In standard ferroelectrics, n is of course the temperature T . For a derivation of the Curie-Weiss law with $n \equiv T$ induced by giant phonon anharmonicity (as in many thermoelectric materials⁵¹) see Ref.⁵². In ferroelectric-type SCs, n could be electron doping¹⁴ or the mechanical strain¹⁵, $n \equiv \epsilon$. In both cases, the variation of the control parameter n changes the phonon damping Γ , as mentioned above.

Using Eq.(3) together with Eq.(2), we solve for the damping and obtain the following relationship:

$$\Gamma(n) = 2\sqrt{\omega_0^2 - |n_c - n|}. \quad (4)$$

The energy of the mode (real part of the frequency, Eq.(3)) and the inverse lifetime (imaginary part, Eq.(4)) are plotted in Fig.1 for the choice $\omega_0 = 0.5$, $n_c = 1$.

It is important to stress that the Curie law in Eq.(3) is valid only close to the instability $n \sim n_c$ and it cannot be trusted far away from there. This is also evident from the expression for the damping in Eq.(4) which stops to be real outside the window $|n_c - \omega_0^2| < n < n_c + \omega_0^2$. As a matter of fact, we will consider the external parameter n only within that range in the rest of the manuscript.

B. Gap equation with anharmonic phonon damping

We briefly recall the anharmonic BCS framework of Ref.³⁶. We will assume a large electron density limit

without explicitly taking into account strong coupling effects which may be relevant to the specific case of SrTiO_3 ¹³. For a generic Fermionic Matsubara frequency ω_n and momentum \mathbf{k} , we denote the superconducting gap function as $\Delta(i\omega_m, \mathbf{k})$. We assume throughout a quadratic nearly-free electron dispersion relation for the electronic band. With a constant coupling g , the gap equation can be derived from the Eliashberg equations in the one-loop (weak coupling) approximation, and takes the form^{53,54}

$$\Delta(i\omega_n, \mathbf{k}) = \frac{g^2}{\beta V} \sum_{\mathbf{q}, \omega_m} \frac{\Delta(i\omega_m, \mathbf{k} + \mathbf{q}) \Pi(\mathbf{q}, i\omega_n - i\omega_m)}{\omega_m^2 + \xi_{\mathbf{k}+\mathbf{q}}^2 + \Delta(i\omega_m, \mathbf{k} + \mathbf{q})^2}, \quad (5)$$

where β is the inverse temperature and V is the volume. In Matsubara frequency space, we choose the pairing mediator to be a damped optical phonon given by the bosonic propagator⁵⁵

$$\Pi(\mathbf{q}, i\Omega_n) = \frac{1}{\Omega(q)^2 + \Omega_n^2 + \Gamma(q)\Omega_n}. \quad (6)$$

Here Ω_n is the bosonic Matsubara frequency for the phonon, $\Omega(q) = \omega_0$ is the frequency of the optical phonon. For our initial treatment, we neglect any dispersion effects of the optical phonon. We take the damping $\Gamma(q)$ equal to Eq.(4) in order to account for the effect of the soft mode. As the phonon mode is optical, we choose no additional dispersion effects in the damping coefficient⁵⁶.

Assuming an isotropic, frequency-independent gap $\Delta(i\omega_n, \mathbf{k}) \equiv \Delta$, we set the external frequency and momentum to zero without any loss of generality. Converting the resulting summation into an energy integral (and assuming a quadratic dispersion relation for the fermions), the gap equation becomes

$$1 = \sum_m \int_{-\infty}^{\infty} \frac{\lambda T d\xi}{[\omega_0^2 + \Omega_m^2 - \Gamma\Omega_m] [\omega_m^2 + \xi^2 + \Delta^2]}, \quad (7)$$

where the chemical potential is considered to be large so that the lower limit of the energy integral is taken to negative infinity. We also define the effective coupling constant $\lambda = N(0)g^2$ and $N(0)$ is the density of states at the Fermi level. We can now perform the energy integral exactly in the limit of large chemical potential to obtain a simplified gap equation. The condition for T_c can then be evaluated by setting $\Delta = 0$ to get

$$1 = \sum_{m=-\infty}^{\infty} \frac{\bar{\lambda}}{2|m + \frac{1}{2}|(m^2\bar{T}_c^2 - m\bar{\Gamma}\bar{T}_c + 1)}. \quad (8)$$

Here $\bar{T}_c \equiv \frac{T_c}{\omega_0}$, $\bar{\Gamma} \equiv \frac{\Gamma}{\omega_0}$ and $\bar{\lambda} \equiv \frac{\lambda}{\omega_0}$ are the critical temperature, damping and the effective coupling constant normalized by the phonon frequency. Performing the Matsubara sum using methods described in Ref.⁵⁷ leads to an equation for T_c that can be numerically solved. This condition is given as

$$4 \left(1 - \frac{4\gamma\bar{\lambda}}{2\bar{\Gamma}\bar{T}_c + \bar{T}_c^2 + 4} - \frac{4\log(4)\bar{\lambda}}{2\bar{\Gamma}\bar{T}_c + \bar{T}_c^2 + 4} - \frac{\bar{\lambda}\psi^{(0)}\left(\frac{\bar{\Gamma}}{2\bar{T}_c} - \frac{\sqrt{\bar{\Gamma}^2-4}}{2\bar{T}_c} + 1\right)}{\bar{T}_c\sqrt{\bar{\Gamma}^2-4} - \bar{\Gamma}^2 + \bar{\Gamma}\sqrt{\bar{\Gamma}^2-4} + 4} - \frac{\bar{\lambda}\psi^{(0)}\left(\frac{\sqrt{\bar{\Gamma}^2-4}}{2\bar{T}_c} - \frac{\bar{\Gamma}}{2\bar{T}_c}\right)}{\bar{T}_c\sqrt{\bar{\Gamma}^2-4} - \bar{\Gamma}^2 + \bar{\Gamma}\sqrt{\bar{\Gamma}^2-4} + 4} \right. \\ \left. + \frac{\bar{\lambda}\psi^{(0)}\left(-\frac{\bar{\Gamma}}{2\bar{T}_c} - \frac{\sqrt{\bar{\Gamma}^2-4}}{2\bar{T}_c}\right)}{\bar{T}_c\sqrt{\bar{\Gamma}^2-4} + \bar{\Gamma}^2 + \bar{\Gamma}\sqrt{\bar{\Gamma}^2-4} - 4} + \frac{\bar{\lambda}\psi^{(0)}\left(\frac{\bar{\Gamma}}{2\bar{T}_c} + \frac{\sqrt{\bar{\Gamma}^2-4}}{2\bar{T}_c} + 1\right)}{\bar{T}_c\sqrt{\bar{\Gamma}^2-4} + \bar{\Gamma}^2 + \bar{\Gamma}\sqrt{\bar{\Gamma}^2-4} - 4} \right) = 0, \quad (9)$$

where $\psi^{(0)}(x)$ is the digamma function and γ is the Euler constant.

The solution of the gap equation, Eq. 9, for \bar{T}_c as a function of $\bar{\Gamma}$ is plotted in Fig. 2. The curves exhibit two kinds of behaviors. The first is a monotonically increasing behavior of \bar{T}_c for small $\bar{\lambda}$ (red curve). The second is a non-monotonic behavior of \bar{T}_c with $\bar{\Gamma}$ for larger $\bar{\lambda}$ (blue curve). In both cases, there is no solution for superconductivity for large enough $\bar{\Gamma} \gtrsim 1$, although the exact critical value is different for various $\bar{\lambda}$. The behavior of the \bar{T}_c curves for different $\bar{\lambda}$ can be understood in several ways. First, we note that there are two types of Matsubara frequency transfers that play a role in the gap Eq. 8: pos-

itive ($m > 0$, Stokes) and negative ($m < 0$, anti-Stokes) contributions. The scattering amplitudes between the electrons and the Stokes (anti-Stokes) phonons is enhanced (reduced) by damping effects from the denominator of the gap equation. Hence, for a given coupling $\bar{\lambda}$ and damping $\bar{\Gamma}$, Stokes (anti-Stokes) phonons lead to a larger (smaller) pair binding between electrons and require a larger (smaller) critical temperature to satisfy the gap equation. For small $\bar{\lambda}$, the Stokes scattering dominates for all $\bar{\Gamma}$ and a monotonically increasing \bar{T}_c is obtained. But for larger $\bar{\lambda}$, there is a competition between the Stokes and anti-Stokes scatterings leading to a minimum in \bar{T}_c at non-zero $\bar{\Gamma}$. The behavior of the \bar{T}_c curves

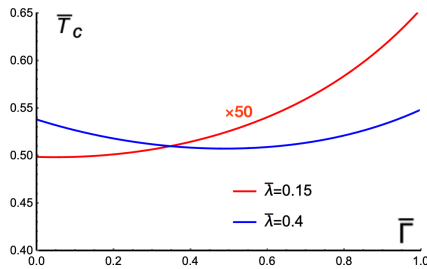


FIG. 2. Plot of normalized critical temperature with damping Γ for different effective couplings $\bar{\lambda}$. For large values of $\bar{\Gamma}$, there is no solution for superconductivity.

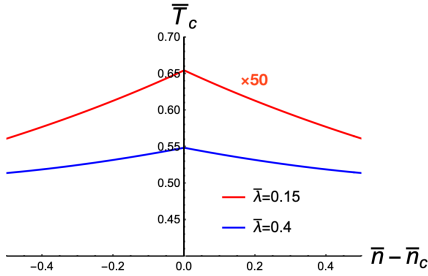


FIG. 3. Plot of normalized critical temperature around the ferroelectric critical point $\bar{n} - \bar{n}_c$ for different effective couplings $\bar{\lambda}$.

can also be understood from a perturbative expansion of the gap equation for small $\bar{\Gamma}$ up to second order in $\bar{\Gamma}$. The linear order term $O(\bar{\Gamma})$ is sensitive to electron scattering from Stokes and anti-Stokes phonons with the latter contributions dominating to cause a decrease in \bar{T}_c . On the other hand, the quadratic $O(\bar{\Gamma}^2)$ term is always positive and mostly insensitive to the sign of the phonon energy exchange acting to enhance pair binding and \bar{T}_c . Below a critical $\bar{\lambda}$, the $O(\bar{\Gamma}^2)$ dominates over $O(\bar{\Gamma})$ for all $\bar{\Gamma}$ giving a monotonic increase in \bar{T}_c , while for larger $\bar{\lambda}$ the two orders compete resulting in a minimum of \bar{T}_c at a finite $\bar{\Gamma}$. The lack of superconductivity for large $\bar{\Gamma}$ can be understood by taking the limit $\bar{\Gamma} \gg 1$ in Eq. 8. In this limit, the leading order contribution to the gap equation diverges for $m = 0$ and hence there is no solution for T_c possible.

III. RESULTS

A. Emergence of the superconducting dome

Upon using Eq. (4) for the damping coefficient $\Gamma(n)$ in Eq. (9) and solving numerically, we can study the evolution of T_c as a function of the external control parameter n that drives the ferroelectric transition. The trend is shown in Fig. 3. Clearly the theoretical calculations display a superconducting dome centered on the soft mode at $n = n_c$. In particular, the T_c grows with approaching

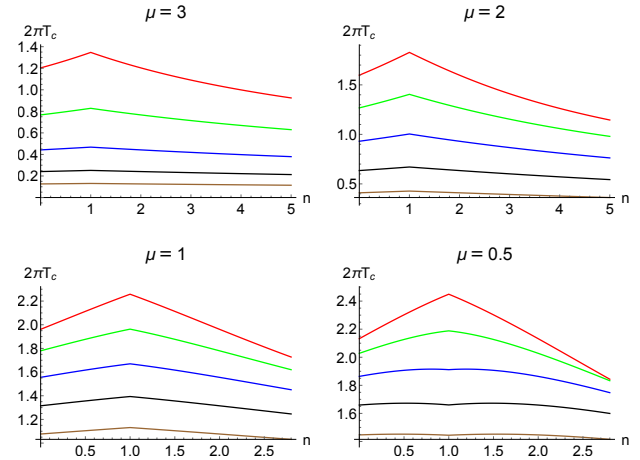


FIG. 4. Superconducting dome predicted by the anharmonic theoretical model with a dispersion of the soft phonon quadratic in momentum transfer, i.e. $\Omega(q) = \omega_0 + \alpha q^2$, where coefficient α is the stiffness or “velocity”. T_c is plotted as a function of the soft phonon control parameter n upon approaching the soft mode instability at $n = n_c = 1$. In each plot, curves are plotted for the following values of the optical energy ω_0 , from top to bottom: $\omega_0 = 0.3, 0.4, 0.5, 0.6, 0.7$. In each plot, the chemical potential μ is fixed to the value shown.

the soft mode instability towards $n = n_c$ on both sides, i.e. both above and below n_c ; or in other words, both in the ferroelectric and in the paraelectric phase. A physical explanation for this widely observed behavior^{10,14,15} is thus offered by the structure of our model.

The mechanism giving rise to the T_c trend in Fig. 3 can be understood in the following manner. By considering Fig. 1, it is clear that the damping Γ grows with approaching $n = n_c$ on both sides of the transition, in qualitative agreement with experiments on ferroelectrics⁵⁸. As n approaches n_c in Eq. 4, $\bar{\Gamma}$ becomes larger and approaches a value of $O(1)$. In the vicinity of this limit, \bar{T}_c increases with increasing $\bar{\Gamma}$ regardless of the coupling $\bar{\lambda}$ (see Fig. 2). Hence, this correlation of T_c with Γ near the critical point leads to a reduction of T_c away from n_c when $\bar{\Gamma}$ decreases. The resulting dome-like behavior of T_c vs n is shown in Fig. 3. The dome like feature is therefore ultimately tied to the dominant, damping-assisted, Stokes scattering processes which act as to increase T_c , by overcoming the de-pairing effects from anti-Stokes processes. This regime also coincides with a value of $\bar{\Gamma}$ that is small enough to perform a perturbative series expansion in the parameter $\bar{\Gamma} < 1$, but also large enough so that second order ($O(\bar{\Gamma}^2)$) damping processes dominate over the linear order terms ($O(\bar{\Gamma})$) in the gap equation. The second order processes lead to a T_c enhancement as described in the previous section.

The physics of ferroelectric superconductors described above must be contrasted with previously studied anharmonic^{35,36} or glassy⁵⁹ systems where the pairing mediator contains a non-trivial spatial stiffness term associated with some dispersive q -dependence of the phonon. First,

due to the key role of acoustic phonons in those studies, a non-trivial spatial stiffness is important to achieve enhanced T_c with damping or decoherence. In the current scenario where the damping coefficient $\bar{\Gamma}$ is independent of momentum transfer due to the nature of the optical mode, a non-trivial spatial stiffness is not necessary to achieve T_c enhancement with $\bar{\Gamma}$. Second, the mechanism of T_c enhancement in damped acoustic or glassy systems involves a constructive interference either between low and high energy phonons or Stokes–anti-Stokes processes. In the current theory we propose for ferroelectric materials, the T_c enhancement occurs mainly from dominant Stokes processes while anti-Stokes processes are detrimental to superconductivity. Finally, the central role of a non-trivial spatial stiffness in Cooper pairing mediated by acoustic, optical or glassy modes is to enhance superconductivity for perturbatively *weak* anharmonic decoherence only (even for intermediate $\bar{\lambda}$). While T_c peaks at an optimal damping scale, set by the spatial stiffness of the bosonic mode, it is gradually suppressed for very strong damping. Consequently, the anticorrelation between strong damping and superconductivity gives a dip in T_c at n_c rather than a dome, not quite consistent with experiments in ferroelectric materials. We therefore do not anticipate a central role for a pairing propagator with finite spatial stiffness (due to non-trivial phonon dispersion in momentum space), for understanding superconductivity in ferroelectric materials near a ferroelectric critical point. In the current proposal, however, T_c is enhanced for strong enough damping with an abrupt loss of superconductivity above a critical damping set by $\bar{\lambda}$, thus yielding the necessary experimental dependence on n . Therefore, material design principles that aim to realize this effect experimentally in other realistic superconducting ferroelectric systems can be guided by regions of the phase diagram with significantly damped bosonic modes. A weak coupling constant (well within the BCS limit), in addition, ensures that T_c monotonically increases with damping up to a critical value, hence ensuring a peak at the critical point.

Before we conclude, for the sake of completeness we briefly discuss the possibility of obtaining the experimental T_c curves near n_c in the weak dissipation limit and intermediate $\bar{\lambda}$. This requires a T_c enhancement with dissipation at $\bar{\lambda} \sim 0.5$. Under this working assumption, we must include a dispersion term of the optical phonon which is quadratic in the momentum transfer q with a prefactor coefficient α that sets the stiffness or “veloc-

ity”³⁶, i.e. $\Omega(q) = \omega_0 + \alpha q^2$. Numerically evaluating the gap equation as a function of $n - n_c$, we plot the resulting T_c behavior in Fig. 4. An explicit dependence on the chemical potential μ appears due to the quadratic dispersion term of the optical phonon. While the role of μ is to reduce the overall scale of T_c (the chemical potential acts like a mass term and hence reduces T_c), the general dome-like trend of T_c with n is preserved for small enough ω_0 . For large ω_0 and small μ , the dome gives way to a shallow dip in T_c at the critical point.

IV. CONCLUSION

We presented a theory of superconductivity enhanced by anharmonic damping in ferroelectric-type materials based on a minimal agnostic model for the soft mode instability. The key effect driving the enhancement of T_c at the soft mode transition is the anharmonic phonon damping which increases upon approaching the transition on both sides, hence the ubiquitous dome. The dome-like feature stems from the dominant, damping-assisted, Stokes scattering processes which act as to increase T_c , by overcoming the de-pairing effects from anti-Stokes processes. Treating the damping effects perturbatively, we showed that the quadratic order damping processes are key to enhancing the pairing as opposed to linear order terms. This explains the crucial role of phonon anharmonic damping near the ferroelectric soft mode to obtain the experimentally observed behavior of T_c , which is supported by gigantic values of anharmonic Grüneisen parameter observed in these systems¹⁵. The presented theory explains the widely observed dome in T_c observed at ferroelectric-type transitions purely in terms of lattice dynamics and phonon physics, and without the need of invoking any exotic electronic effects. Furthermore, it provides useful guidelines for material-by-design rules to engineer ferroelectric-type materials with optimized superconducting properties.

Acknowledgements – M.B. acknowledges the support of the Shanghai Municipal Science and Technology Major Project (Grant No.2019SHZDZX01). C.S. is supported by the U.S. DOE grant number DE-FG02-05ER46236. A.Z. acknowledges financial support from US Army Research Laboratory and US Army Research Office through contract nr. W911NF-19-2-0055.

* csetty@ufl.edu

† b.matteo@sjtu.edu.cn

‡ alessio.zaccone@unimi.it

¹ B. T. Matthias, Physical review **97**, 74 (1955).

² P. W. Anderson and E. Blount, Physical Review Letters **14**, 217 (1965).

³ J. Appel, Physical Review Letters **17**, 1045 (1966).

⁴ J. Appel, Physical Review **180**, 508 (1969).

⁵ V. L. Ginzburg, Ferroelectrics **76**, 3 (1987), <https://doi.org/10.1080/00150198708009019>.

⁶ A. Bussmann-Holder, A. Simon, and H. Büttner, Physical Review B **39**, 207 (1989).

⁷ G. Binnig, A. Baratoff, H. E. Hoenig, and J. G. Bednorz, *Phys. Rev. Lett.* **45**, 1352 (1980).

⁸ C. Enderlein, J. F. de Oliveira, D. A. Tompsett, E. B. Saitovitch, S. S. Saxena, G. G. Lonzarich, and S. E. Rowley, *Nature Communications* **11**, 4852 (2020).

⁹ C. Koonce, M. L. Cohen, J. Schooley, W. Hosler, and E. Pfeiffer, *Physical Review* **163**, 380 (1967).

¹⁰ J. M. Edge, Y. Kedem, U. Aschauer, N. A. Spaldin, and A. V. Balatsky, *Phys. Rev. Lett.* **115**, 247002 (2015).

¹¹ J. F. Schooley, W. R. Hosler, and M. L. Cohen, *Phys. Rev. Lett.* **12**, 474 (1964).

¹² X. Lin, Z. Zhu, B. Fauqué, and K. Behnia, *Phys. Rev. X* **3**, 021002 (2013).

¹³ A. V. Chubukov, I. Eremin, and D. V. Efremov, *Physical Review B* **93**, 174516 (2016).

¹⁴ J. Ma, R. Yang, and H. Chen, *Nature Communications* **12**, 2314 (2021).

¹⁵ J. Franklin, B. Xu, D. Davino, A. Mahabir, A. V. Balatsky, U. Aschauer, and I. Sochnikov, *Phys. Rev. B* **103**, 214511 (2021).

¹⁶ S. Hameed, D. Pelc, Z. W. Anderson, A. Klein, R. J. Spieker, L. Yue, B. Das, J. Ramberger, M. Lukas, Y. Liu, M. J. Krogstad, R. Osborn, Y. Li, C. Leighton, R. M. Fernandes, and M. Greven, *Nature Materials* (2021), 10.1038/s41563-021-01102-3.

¹⁷ M. N. Gastiasoro, J. Ruhman, and R. M. Fernandes, *Annals of Physics* **417**, 168107 (2020).

¹⁸ J. Ruhman and P. A. Lee, *Phys. Rev. B* **94**, 224515 (2016).

¹⁹ Y. Yu, H. Y. Hwang, S. Raghu, and S. B. Chung, arXiv e-prints , arXiv:2110.03710 (2021), arXiv:2110.03710 [cond-mat.supr-con].

²⁰ B. Rosenstein and B. Y. Shapiro, *Phys. Rev. B* **100**, 054514 (2019).

²¹ J. Phillips, *Physics of High-Tc Superconductors* (Academic Press, 1989) pp. 1–25.

²² B. Rosenstein and B. Y. Shapiro, *Journal of Physics Communications* **5**, 055013 (2021).

²³ D. Sun, V. S. Minkov, S. Mozaffari, S. Chariton, V. B. Prakapenka, M. I. Eremets, L. Balicas, and F. F. Balakirev, arXiv e-prints , arXiv:2010.00160 (2020), arXiv:2010.00160 [cond-mat.supr-con].

²⁴ X.-J. Chen, *Matter and Radiation at Extremes* **5**, 068102 (2020), https://doi.org/10.1063/5.0033143.

²⁵ T. B. Rawal, L.-H. Chang, H.-D. Liu, H.-Y. Lu, and C. S. Ting, arXiv e-prints , arXiv:2110.00105 (2021), arXiv:2110.00105 [cond-mat.supr-con].

²⁶ M. V. Sadovskii, arXiv e-prints , arXiv:2106.09948 (2021), arXiv:2106.09948 [cond-mat.supr-con].

²⁷ L. R. Testardi, *Rev. Mod. Phys.* **47**, 637 (1975).

²⁸ M. Le Tacon, A. Bosak, S. M. Souliou, G. Dellea, T. Loew, R. Heid, K.-P. Bohnen, G. Ghiringhelli, M. Krisch, and B. Keimer, *Nature Physics* **10**, 52 (2014).

²⁹ H. Uchiyama, A. Q. R. Baron, S. Tsutsui, Y. Tanaka, W.-Z. Hu, A. Yamamoto, S. Tajima, and Y. Endoh, *Phys. Rev. Lett.* **92**, 197005 (2004).

³⁰ M. d’Astuto, G. Dhaliinne, J. Graf, M. Hoesch, P. Giura, M. Krisch, P. Berthet, A. Lanzara, and A. Shukla, *Phys. Rev. B* **78**, 140511 (2008).

³¹ D. Reznik, T. Fukuda, D. Lamago, A. Baron, S. Tsutsui, M. Fujita, and K. Yamada, *Journal of Physics and Chemistry of Solids* **69**, 3103 (2008), sNS2007.

³² W. S. Lee, K.-J. Zhou, M. Hepting, J. Li, A. Nag, A. C. Walters, M. Garcia-Fernandez, H. C. Robarts, M. Hashimoto, H. Lu, B. Nosarzewski, D. Song, H. Eisaki, Z. X. Shen, B. Moritz, J. Zaanen, and T. P. Devereaux, *Nature Physics* **17**, 53 (2021).

³³ S. Sarkar, M. Grandadam, and C. Pépin, *Phys. Rev. Research* **3**, 013162 (2021).

³⁴ D. F. Valentinis, C. Berthod, B. Bordini, and L. Rossi, *Superconductor Science and Technology* **27**, 025008 (2013).

³⁵ C. Setty, M. Baggio, and A. Zacccone, *Phys. Rev. B* **102**, 174506 (2020).

³⁶ C. Setty, M. Baggio, and A. Zacccone, *Phys. Rev. B* **103**, 094519 (2021).

³⁷ Y. Mizukami, M. Kończykowski, O. Tanaka, J. Juraszek, Z. Henkie, T. Cichorek, and T. Shibauchi, *Phys. Rev. Research* **2**, 043428 (2020).

³⁸ A. M. Kosevich, *The Crystal Lattice* (John Wiley & Sons, Ltd, Weinheim, 2005) pp. 1–13.

³⁹ P. G. Klemens, *Phys. Rev.* **148**, 845 (1966).

⁴⁰ C. Kittel, *Introduction to solid state physics. Eighth edition* (John Wiley & Sons, 2005).

⁴¹ L. P. Gor’kov, *Proceedings of the National Academy of Sciences* **113**, 4646 (2016).

⁴² M. N. Gastiasoro, T. V. Trevisan, and R. M. Fernandes, *Phys. Rev. B* **101**, 174501 (2020).

⁴³ M. N. Gastiasoro, M. Eleonora Temperini, P. Barone, and J. Lorenzana, arXiv e-prints , arXiv:2109.13207 (2021), arXiv:2109.13207 [cond-mat.supr-con].

⁴⁴ D. van der Marel, F. Barantani, and C. W. Rischau, *Phys. Rev. Research* **1**, 013003 (2019).

⁴⁵ P. A. Volkov, P. Chandra, and P. Coleman, arXiv e-prints , arXiv:2106.11295 (2021), arXiv:2106.11295 [cond-mat.supr-con].

⁴⁶ D. Kiseliov and M. Feigel’man, arXiv e-prints , arXiv:2106.09530 (2021), arXiv:2106.09530 [cond-mat.supr-con].

⁴⁷ K. L. Ngai, *Phys. Rev. Lett.* **32**, 215 (1974).

⁴⁸ Y. Xu, J.-S. Wang, W. Duan, B.-L. Gu, and B. Li, *Phys. Rev. B* **78**, 224303 (2008).

⁴⁹ T. Tadano and S. Tsuneyuki, *Journal of the Physical Society of Japan* **87**, 041015 (2018), https://doi.org/10.7566/JPSJ.87.041015.

⁵⁰ T. Tadano and S. Tsuneyuki, *Phys. Rev. B* **92**, 054301 (2015).

⁵¹ C. W. Li, J. Hong, A. F. May, D. Bansal, S. Chi, T. Hong, G. Ehlers, and O. Delaire, *Nature Physics* **11**, 1063 (2015).

⁵² L. Casella and A. Zacccone, *Journal of Physics: Condensed Matter* **33**, 165401 (2021).

⁵³ F. Marsiglio and J. Carbotte, in *Superconductivity* (Springer, 2008) pp. 73–162.

⁵⁴ H. Kleinert, *Collective classical and quantum fields* (World Scientific, Singapore, 2018).

⁵⁵ J. M. Ziman, *Elements of Advanced Quantum Theory* (Cambridge University Press, Cambridge, 1969).

⁵⁶ P. Klemens, *Physical Review* **148**, 845 (1966).

⁵⁷ A. Larkin and A. Varlamov, *Theory of fluctuations in superconductors* (Clarendon Press, 2005).

⁵⁸ T. Lanigan-Atkins, S. Yang, J. L. Niedziela, D. Bansal, A. F. May, A. A. Puretzky, J. Y. Y. Lin, D. M. Pajerowski, T. Hong, S. Chi, G. Ehlers, and O. Delaire, *Nature Communications* **11**, 4430 (2020).

⁵⁹ C. Setty, *Phys. Rev. B* **99**, 144523 (2019).